Photoluminescence from the $^5D_0$ level of Eu^{3+} ions in a phosphate glass under pressure

Photoluminescence from the $^5D_0$ level of Eu^{3+} ions in a phosphate glass under pressure

S Surendra Babu[1], **P Babu**[1], **C K Jayasankar**[1,4], **Th Tröster**[2], **W Sievers**[3] **and G Wortmann**[3]

[1] Department of Physics, Sri Venkateswara University, Tirupati-517 502, India
[2] University of Applied Sciences, Faculty of Automotive Systems and Production, D-50679 Cologne, Germany
[3] Department Physik, Universität Paderborn, D-33095 Paderborn, Germany

E-mail: ckjaya@yahoo.com

Abstract
The pressure dependence of the luminescence from $^5D_0 \rightarrow {}^7F_{0,1,2}$ transitions of Eu^{3+} ions in $58.5P_2O_5$–$9Al_2O_3$–$14.5BaO$–$17K_2O$–$1Eu_2O_3$ glass has been investigated up to 38.3 GPa at room temperature. The relative luminescence intensity ratio of $^5D_0 \rightarrow {}^7F_2$ to $^5D_0 \rightarrow {}^7F_1$ transitions of the Eu^{3+} ions is found to decrease with increasing pressure, indicating a lowering of the asymmetry around the Eu^{3+} ions with pressure. The $^5D_0 \rightarrow {}^7F_{0,1,2}$ transitions exhibit pressure-induced red shifts of different magnitude, which suggests a decrease in Slater parameters (F^k) and in the spin–orbit coupling parameters (ζ) for the Eu^{3+} ions. Stark components of the $^7F_1$ level have been used to evaluate the crystal-field (CF) parameters B_{20} and B_{22}, which are in turn used to estimate the CF strength experienced by the Eu^{3+} ions in the glass. The observed increase in the CF strength parameter is found to have an almost cubic dependence on pressure. Luminescence decay curves for the $^5D_0 \rightarrow {}^7F_2$ transition are found to be single exponential over the entire pressure range studied. The lifetime did not change under pressure up to 5 GPa, although a significant change in the CF strength is noticed in this pressure range. The reduction of lifetime observed at pressures above 5 GPa could be partially due to an increase of pressure-induced defect centres. Such a process can then explain the hysteresis observed in the variation of lifetime and crystal-field strength on the release of pressure.

1. Introduction

Lanthanide (Ln) doped phosphate based glasses have been the subject of recent investigations as potential materials for luminescent applications. Typically, phosphate based multi-oxide

glasses possess high stimulated emission cross-sections, weak up-conversion luminescence and low probability of energy back transfer. In addition, these glasses exhibit high transparency, low refractive index, low melting temperature, high gain, good thermo-optical performance, low rupture strength and good chemical durability [1–4]. When a Ln ion is incorporated into any host matrix, it experiences an inhomogeneous crystal field produced by the surrounding charge distribution and results in two effects which are the centroid shifts of all the free-ion multiplets to the red and the Stark splitting of the energy levels. The centroid shifts are ascribed as the Nephelauxetic effect that explains the reduction of Slater parameters (F^k) and the spin–orbit coupling parameter (ζ) for the Ln ion in the host with respect to their free-ion values of F_k^0 and ζ^0. The Stark splitting of the multiplets is ascribed to the change in the sum of various interactions such as covalence, overlap and Coulomb interactions between the 4f electrons of the Ln ions and their surrounding ligands. These two effects significantly influence the luminescence properties of Ln ions in the solids.

The development of luminescence materials for practical applications such as solid state lasers, optical data storage devices, optical sensors, and phosphors requires a systematic understanding of bonding environment of Ln ions and their luminescence properties. Application of high pressure continuously reduces the interatomic distance and therefore increases the overlap among the adjacent electronic orbitals and the crystal-field (CF) strength, without changing the other physical properties like the point group symmetry of the Ln ion site or the chemical composition. The decrease in the effective volume of the Ln ion containing matrix with high pressure has different effects on different luminescence centres. Thus, a pressure dependent luminescence study provides precise information on the electronic states, CF strength, energy transfers and the interaction between luminescence centres and their hosts [5].

Glasses doped with trivalent europium (Eu^{3+}) ions have been used in optical devices as red emitting materials for field emission technology, phosphors and LEDs which exhibits longer luminescence efficiency [6–9]. Apart from these potential luminescent applications, $Eu^{3+}(4f^6)$ ions have often been used as a probe to estimate the local environment around the Ln^{3+} ions in different materials. The information about the local structure around a Eu^{3+} ion can be obtained quite easily from its f–f transition spectra. The luminescence of Eu^{3+} ions also facilitates estimating the precise information about the non-uniformity of Eu^{3+} ion sites and the strength of Eu–O bonding. The ground state $^7F_0$ and the first excited $^5D_0$ states of Eu^{3+} are non-degenerate under any symmetry and some of the transitions between these levels are sensitive to the local environment. Hence, information regarding the local environment around the Eu^{3+} ion is contained in the $^5D_0 \rightarrow {}^7F_J$ emission transitions and their splitting. Depending on the number of Stark components into which the $^5D_0 \rightarrow {}^7F_J$ emission transitions split, the symmetry at the Eu^{3+} site can be derived by crystal-field parameterization. The crystal-field parameters B_{20} and B_{22} as well as their ratio have been used to describe the coordination of the Eu^{3+} ions [10–12]. Thus, Eu^{3+} ion luminescence spectroscopy can be used as a technique to study the effect of pressure on the structure of an amorphous material. The present work reports the results of luminescence spectra of $^5D_0 \rightarrow {}^7F_{0,1,2}$ transitions and lifetime measurements of the $^5D_0$ level of Eu^{3+} ion in a phosphate glass under high pressure up to 38.3 GPa at room temperature with the aim of using the high pressure technique to investigate the pressure induced changes in the luminescence properties of Eu^{3+} ions in the phosphate glass. The effect of a pressure release on these properties is also studied.

2. Experimental details

The Eu^{3+} doped phosphate based multi-oxide glass with composition (in mol%) of $58.5P_2O_5$–$17 K_2O$–$14.5 BaO$–$9Al_2O_3$–$1Eu_2O_3$ (PKBAEu) was prepared by a conventional

melt quenching technique. About 5 g of the batch composition was thoroughly crushed in an agate mortar and the homogeneous mixture was heated in a platinum crucible inside an electric furnace for 45 min at a temperature of 1075 °C. The melt was poured onto a preheated brass mould at a temperature of 350 °C and annealed at this temperature for about 5 h to remove thermal strains. Then the sample was allowed to cool to room temperature (RT) and polished for the purpose of optical measurements.

The 465.8 nm line of an Ar$^+$ laser was used as excitation source. The fluorescence spectra were recorded with a double monochromator equipped with a photomultiplier tube. The resolution of the double monochromator expressed in nanometres depends on the wavelength and on the slit width. Evaluated in wavenumbers, the resolution was typically set to 2.0 cm^{-1} over the whole range covered. A special miniature diamond anvil cell (DAC) was used to generate pressures up to nearly 40 GPa at RT. A piece of the PKBAEu glass was placed together with a ruby pressure sensor in an 80 μm diameter hole of a stainless steel (INCONEL X750) gasket of 200 μm thickness. A mixture of methanol:ethanol:water (16:3:1) was used as the pressure transmitting medium. This gasket with the sample and pressure transmitting fluid was then compressed by the two opposed anvils of the DAC. The pressure and the hydrostatic conditions experienced by the sample were determined by the shift and broadening of the ruby R_1 lines [13]. A mechanical chopper in connection with a multi-channel scalar allowed for lifetime measurement in the range from 2 μs to 2 s.

3. Crystal-field analysis

When a free-ion is introduced into a solid, it experiences an inhomogeneous crystal field produced by the surrounding charge distribution. The Hamiltonian that represents the CF potential acting on the Ln ion can be expressed in Wybourne's notation [14–16] as

$$H_{CF} = \sum_{k,q,i} B_q^k C_q^{(k)}(i) \tag{1}$$

where $B_q^k = (-1)^q (B_q^k - i S_q^k)$ are the coefficients of the CF expansion, representing the functions of the radial distances that can be varied in order to match calculated and experimental CF levels. The $C_q^{(k)}$ are tensor operators of rank k, closely related to the spherical harmonics, which can be calculated exactly [15]. The number of parameters for H_{CF} in equation (1) is greatly reduced by the symmetry selection rules for the point symmetry at the Ln site in the crystal. Although the term 'crystal' has been used here, these effects are not confined only to crystals. Any surrounding that breaks the spherical symmetry of the free ion can lead to a shift and splitting of the energy levels. Thus, the above considerations also apply to materials such as glasses where a long-range order does not exist [5].

If the J-mixing effects are neglected, then the CF splitting of the $^7F_1$ level of the Eu^{3+} ion will depend only on the even CF parameters of second rank ($k = 2$).

The observed number of crystal-field levels in a $J = 1$ level ($^7F_1$ and $^5D_1$) gives an indication for the symmetry class of the lanthanide ion site. The $J = 1$ level will not split in a cubic crystal field and the three-fold degeneracy remains. It will split into two levels (a non-degenerate and a two-fold crystal-field level) in the presence of a hexagonal, trigonal or tetragonal crystal field. An orthorhombic, monoclinic or a triclinic crystal field will remove all crystal-field degeneracy and three crystal-field levels can be observed. In this way it is possible to detect distortions in the crystal lattice at the lanthanide ion site. The $^7F_1$ and $^5D_1$ levels are suitable for this because normally all crystal-field levels of these multiplets can be observed experimentally. For the present glass systems at ambient condition as well as under the entire pressure range studied, the $^7F_1$ multiplet shows three well resolved Stark splittings and hence
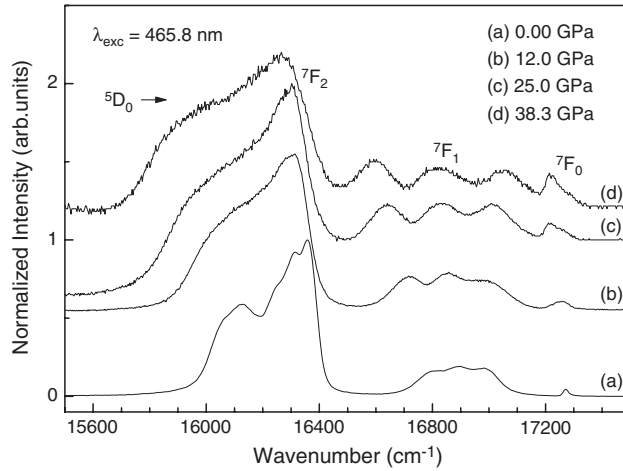
Figure 1. Luminescence spectra of PKBAEu glass at different pressures. The spectra are normalized to the $^5D_0 \rightarrow {}^7F_2$ transition.

the symmetry could be orthorhombic (D_2, C_{2v}), monoclinic (C_2, C_S) or triclinic (C_1) [10]. Further, among these point groups the C_{2v} is the highest point group symmetry that allows complete splitting of all crystal-field components and it has been used extensively in the crystal-field analysis of Eu^{3+} ions in oxide glasses. A detailed explanation for selecting C_{2v} symmetry for Eu^{3+} ions in oxide glasses have been well described by Brecher and Riseberg [17]. For C_{2v} symmetry the 'second-rank crystal field' experienced by Eu^{3+} ions is described by the Hamiltonian as [14]:

$$H_{CF} = B_{20}C_0^{(2)} + B_{22}(C_{-2}^{(2)} + C_2^{(2)})$$ (2)

where B_{20} and B_{22} are the real parts of CF parameters in equation (1).

The CF strength parameter (N_V) has been used to simplify the description of the CF parameters due to its independence from the specific crystal structure. Considering only the second-rank CF parameters, N_V has been determined using the following relation [18]:

$$N_V = \sqrt{\frac{4\pi}{5}((B_{20})^2 + 2(B_{22})^2)}.$$ (3)

4. Results and discussion

A detailed characterization of PKBAEu glass through optical absorption, photoluminescence and decay times using the energy-level model Hamiltonian and Judd–Ofelt theory has been reported in our previous paper [19]. Figure 1 shows the room-temperature photoluminescence spectra of PKBAEu glass for different pressures from ambient up to 38.3 GPa, obtained by excitation at 465.8 nm, along with the band assignments. The spectra correspond to the emission from the $^5D_0$ excited state to the $^7F_{0,1,2}$ ground multiplets of Eu^{3+} ions in PKBAEu glass. The transitions to the ^7F_J states with $J = 3$–6 are of very weak intensity [19] and they could not be observed under high pressure. The $^5D_0 \rightarrow {}^7F_0$, $^7F_1$ and $^7F_2$ are forbidden, magnetic-dipole allowed and enforced electric-dipole allowed transitions, respectively. The transition probability for the magnetic-dipole $^7F_1$ transition is nearly independent of the host matrix. On the other hand, the intensity of the enforced electric-dipole allowed $^7F_2$ transition depends strongly on the Eu^{3+} ion surroundings. Therefore, the luminescence intensity ratio of
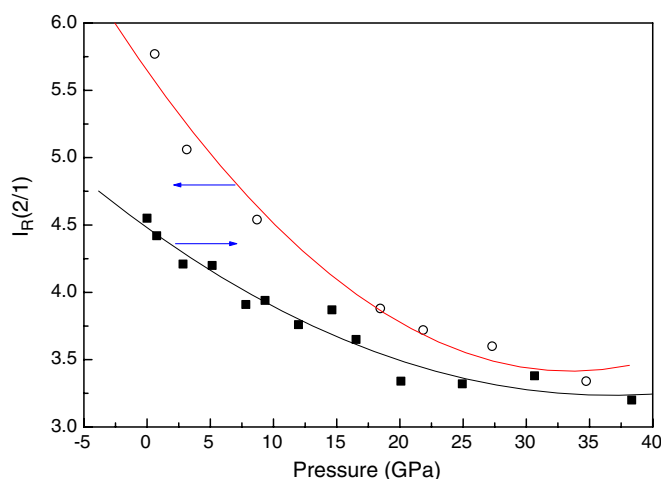
Figure 2. Luminescence intensity ratio $I_R(2/1)$ of the $I(^5D_0 \rightarrow \ ^7F_2)$ to $I(^5D_0 \rightarrow \ ^7F_1)$ transitions as a function of pressure. The solid (open) symbols correspond to data taken at increasing (decreasing) pressure. The curve serves as a guide to the eye. Directions of arrows indicate increase and decrease of pressure.

(This figure is in colour only in the electronic version)

$^5D_0 \rightarrow \ ^7F_2$ to $^5D_0 \rightarrow \ ^7F_1(I_R(2/1))$, widely known as the asymmetric ratio, provides valuable information about the symmetry at the site of the Eu^{3+} ions in any host matrix [20–24]. Moreover, the transition probability of an electric-dipole transition can be expressed in terms of the Judd–Ofelt parameters Ω_λ for Eu^{3+} ions [23, 25]. Hence, the variation of $I_R(2/1)$ and, in turn, Ω_2 provides information about changes of the local structure around Eu^{3+} ions and the Eu–O covalence. The higher the value of $I_R(2/1)$, the higher will be the asymmetry and covalence between Eu^{3+} and its surrounding ligands [19, 20, 24].

Figure 2 shows the variation of $I_R(2/1)$ of PKBAEu glass with pressure. The $I_R(2/1)$ value was found to be 4.6 at ambient pressure, and it decreases to 3.2 when the pressure is increased to 38.3 GPa. Though it is physically not well justified, it is a common practice in the literature [24] to use the factor $I_R(2/1)$ to express the variation of asymmetry in the local environment of Eu^{3+} ions in a given host. Also this kind of pressure induced reduction in the value of $I_R(2/1)$ has been noticed for amorphous $Eu(OH)_3$ by Chen *et al* [22], and they concluded that the pressure induced decrease in the $I_R(2/1)$ value with increasing pressure could be due to either a decrease in the covalence of the Eu–O bonds or a decrease in the average Eu–O bond distance with pressure. From figure 2, it is evident that the $I_R(2/1)$ values are considerably higher while releasing pressure compared to those of increasing pressure. This hysteretic behaviour is exemplified by values obtained at ambient pressure, $I_R(2/1) = 4.55$ before pressure is applied, and $I_R(2/1) = 5.77$, when pressure is released. This observation indicates that after releasing the pressure the asymmetry around the Eu^{3+} ions is higher than at ambient condition, indicating that the increase of local deformation around the Eu^{3+} ion sites after releasing the pressure is due to an increase of pressure induced defect centres.

The disordered structure in the glass causes site-to-site variations in the distances and bonds of the lanthanide ions with their ligands. In the present work, in principle, excitation with the Ar^+ ion laser usually involves a phonon to excite the electronic f levels. Thus, there are always many different sites which are excited. The analysis we are doing is never for a single site but for all sites showing luminescence. Moreover, the ruby pressure sensor (shift
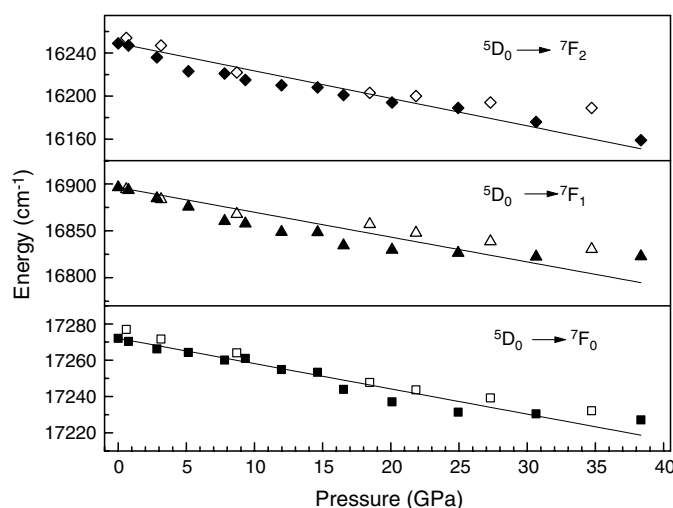
Figure 3. Peak positions of the $^5D_0 \rightarrow$ $^7F_0$, $^7F_1$ and $^7F_2$ transitions of the Eu^{3+} ions in PKBAEu glass as a function of pressure. For the $^5D_0 \rightarrow$ $^7F_1$ transitions, the data points correspond to the barycentre of this transition (see figure 4) and the data points for the $^5D_0 \rightarrow$ $^7F_0$ and $^7F_2$ transitions correspond to the peak maximum. The solid (open) symbols correspond to data taken at increasing (decreasing) pressure. The solid line is the fit of a linear equation of the data obtained at increasing pressure.

and broadening of R_1 and R_2 lines) used to measure the pressure also confirms the uniform hydrostatic pressure condition on the sample so that all sites of the disordered material are under uniform pressure. Thus, we derived the average parameters. However, one may also expect that in the case of monochromatic excitation (even in the case of site selective spectroscopy), it may not permit the energy levels of a single site to be analysed under pressure. This may be due to the fact that the energy levels for excitation of the particular site would shift off-resonance with the single excitation wavelength when the pressure is changed. In such cases, the luminescence band shifts may not reflect the values for the same site since different sites would be excited under different pressure. Figure 3 shows the pressure dependence of the shift of the $^5D_0 \rightarrow$ $^7F_{0,1,2}$ emission band positions of the Eu^{3+} ions along with a linear fit to the data obtained with increasing pressure. The energy positions of these emission bands are taken at the peak maxima of the bands for $^5D_0 \rightarrow$ $^7F_0$ and $^7F_2$ transitions and a barycentre has been taken in the case of the $^5D_0 \rightarrow$ $^7F_1$ transition to avoid ambiguity in determining the peak maximum for this transition. As can be seen from figure 3, the pressure dependent energy level shift can be expressed quite well as a linear function [26, 27]:

$$E_i(p) = E_i(0) + \alpha_i p \qquad \text{(with } p \text{ in GPa)}$$

where i labels the three different transitions. The $E_i(0)$ values correspond to the values at 0.0 GPa and the coefficients α_i are determined from the fits as

$$\alpha(^5D_0 \rightarrow \ ^7F_0) = -1.40 \ cm^{-1}/GPa$$

$$\alpha(^5D_0 \rightarrow \ ^7F_1) = -2.30 \ cm^{-1}/GPa$$

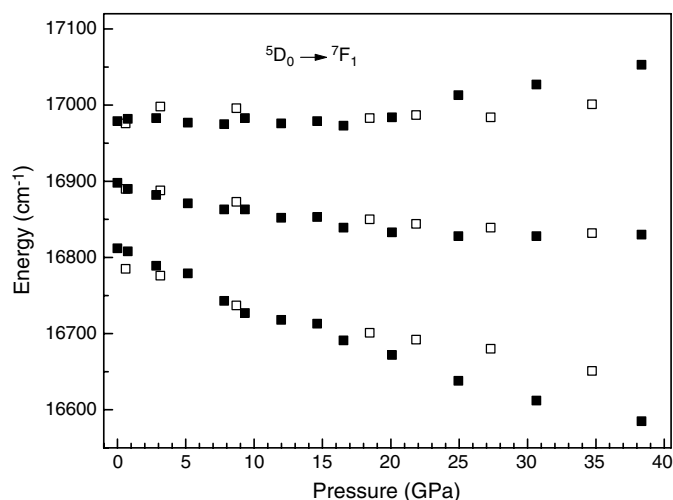$$\alpha(^5D_0 \rightarrow \ ^7F_2) = -2.6 \ cm^{-1}/GPa.$$

Figure 4. Energy positions of the $^5D_0 \rightarrow {}^7F_1$ Stark transitions of Eu^{3+} ions in PKBAEu glass as a function of pressure. The solid (open) symbols correspond to data taken at increasing (decreasing) pressure.

The shift of each J-manifold with pressure results from the reduction of Slater parameters (F^k) and the spin–orbit coupling parameter (ζ) which are due to changes in the overlap of the ligand orbitals with the 4f wavefunctions of the Eu^{3+} ion [28]. Similar red shifts of the $^5D_0 \rightarrow {}^7F_J$ transitions have been observed by Chen *et al* [22] for amorphous $Eu(OH)_3$.

A detailed CF analysis has been carried out to evaluate the CF strength experienced by the Eu^{3+} ion in the host under pressure. The contribution of change in Eu–O bond distance to the decreasing trend of $I_R(2/1)$ with pressure can also be examined with the help of the CF strength experienced by the Eu^{3+} ion in the matrix. Figure 4 shows the three Stark splittings obtained for the $^5D_0 \rightarrow {}^7F_1$ transition of Eu^{3+} ions in the PKBAEu glass under pressure. These Stark energy levels have been obtained by de-convoluting the $^7F_1$ level into three Gaussian line shape functions. As can be seen from figure 4, the observed increase in the energy separation between the two extreme Stark components with increasing pressure quantitatively reflects an increase in the CF strength at the Eu^{3+} ion site under pressure. A more qualitative estimation of the CF strength experienced by the Eu^{3+} ions can be made by the crystal-field parameterization.

The complete removal of degeneracy for the $^5D_0 \rightarrow {}^7F_1$ transition at all pressures suggests that the local symmetry of the Eu^{3+} ions in PKBAEu glass is low, corresponding to orthorhombic, monoclinic or triclinic symmetry in a crystal [14, 15]. From the Stark splittings of the $^5D_0 \rightarrow {}^7F_1$ transition it is possible to estimate the CF strength acting on the Eu^{3+} ions in glasses by assuming C_{2v} site symmetry for the local environment of the Eu^{3+} ions [15–17, 19, 22]. This is because C_{2v} symmetry is a subgroup of almost all higher-order point groups allowing optical activity from the $^5D_0$ level to practically all ^7F_J Stark levels. Furthermore, C_{2v} is the highest order non-centrosymmetric point group that completely lifts the degeneracy of the ^7F_J levels and has the lowest symmetry for which simple crystal-field calculations can be performed routinely. The corresponding second-rank CF parameters, B_{20} and B_{22}, have been calculated by diagonalizing the complete Hamiltonian of the free Eu^{3+} ion and the second-rank crystal-field parameters described in equation (1) assuming C_{2v} symmetry and taking into account the J-mixing as carried out in earlier work [15].
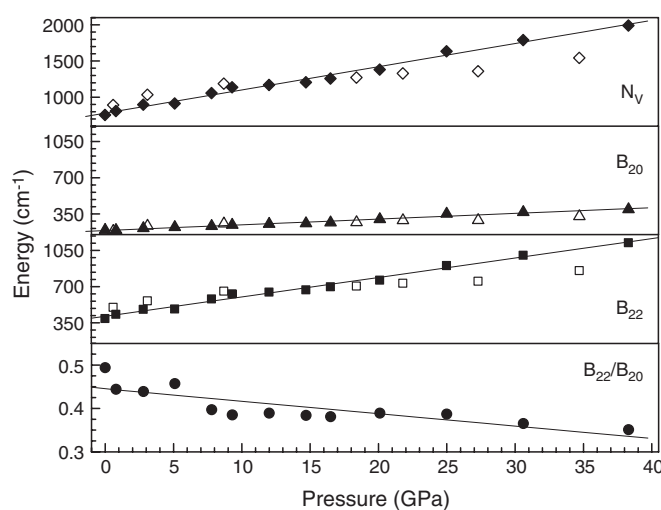
Figure 5. Variation of second-rank crystal-field parameters (B_{20} and B_{22}) and their ratios (B_{22}/B_{20}) and crystal-field strength parameter N_V with pressure. The solid points are the data while increasing the pressure and the open squares are the data while decreasing the pressure (not included for B_{22}/B_{20}). A linear fit of the increasing data is also shown.

The basis set used in the CF calculation consisted of the 65 lowest energy JM_J states (^7F and ^5D multiplets) of the $4f^6$ (Eu^{3+}) configuration [15]. During the energy level fitting, all the 19 free-ion parameters ($F^{2,4,6}$, ζ, α, β, γ, $T^{2,3,4,6,7,8}$, $M^{0,2,4}$, and $P^{2,4,6}$) are fixed to the values of Eu^{3+}:$LaCl_3$ crystal [29]. In order to perform the crystal-field analysis, the free-ion parameters can be fixed to particular values under pressure. This can be done because a slight change in free-ion parameters as arising for example by changing the host or by applying pressure to one and the same host does not significantly affect the behaviour of the crystal-field parameters under pressure. This fact has been used in some cases, where the influence of free-ion parameters has even been ignored (for example, Ln^{3+}:$LnMO_4$ (Ln = Gd, Y, Lu and M = P, As, V) [30]) and in some other cases aquo-ion free-ion parameters (for example, Ln^{3+}:Y_2O_3 [31]) have been taken for crystal-field analysis. In the present work, a well-optimized set of free-ion parameters as derived from the highly reliable energy level scheme of Eu^{3+}:$LaCl_3$ has been used for the crystal-field analysis.

The fitting process minimizes the root mean square deviation between the experimental and calculated $^7F_1$ Stark energy levels. The best fit B_{20} and B_{22} and their ratios (B_{22}/B_{20}) together with the CF strength parameter N_V (defined by equation (3)) are collected in table 1 and are shown in figure 5. The variation of B_{20} and B_{22} as well as of N_V with pressure exhibits, with good statistical accuracy, a linear dependence on pressure. The behaviour of B_{22}/B_{20} has, as the ratio of two derived parameters, less statistical accuracy. It decreases from 0.49 to 0.35 when the pressure is increased from 0.0 to 38.3 GPa. Interestingly, the intensity ratio $I_R(2/1)$ is reduced from 4.55 to 3.20 in the same pressure range by the same ratio. This demonstrates that the local asymmetry around the Eu^{3+} ions is reduced with pressure and that both approaches describing this behaviour are on a physically sound basis.

Also, the fluorescence decay of the $^5D_0 \rightarrow {}^7F_2$ transition in PKBAEu glass has been measured up to 38.3 GPa. The decay profiles are found to be single exponential in the entire pressure range studied. Figure 6 shows the decay profiles at different pressures along with a single exponential fit to the decay profile at 38.3 GPa. Table 1 summarizes the lifetimes of the

Table 1. Energies (cm^{-1}), luminescence intensity ratio of $^5D_0 \rightarrow {}^7F_2$ to $^5D_0 \rightarrow {}^7F_1$, crystal-field parameters and their ratios (B_{20}, B_{22}, B_{22}/B_{20}), crystal-field strength parameter (N_V, cm^{-1}) and $^5D_0$ lifetimes for the PKBAEu glass under (a) increasing pressure and (b) decreasing pressure.

Pressure (GPa)	$^5D_0 \rightarrow {}^7F_0$	$^7F_1$	$^7F_1$	$^7F_1$	$\dfrac{I(^5D_0 \rightarrow {}^7F_2)}{I(^5D_0 \rightarrow {}^7F_1)}$	Lifetime (μs)	B_{20}	B_{22}	B_{22}/B_{20}	N_V
(a) Increasing pressure										
0.0	17 272	16 979	16 898	16 812	4.55	2520	391	193	0.494	756
0.8	17 270	16 982	16 890	16 808	4.42	2508	432	192	0.444	809
2.8	17 266	16 983	16 882	16 789	4.21	2512	480	211	0.439	897
5.1	17 264	16 977	16 871	16 779	4.20	2515	484	221	0.457	913
7.8	17 260	16 975	16 863	16 743	3.91	2375	581	231	0.397	1057
9.3	17 261	16 983	16 863	16 727	3.94	2274	630	243	0.385	1138
12.0	17 255	16 976	16 852	16 718	3.76	2182	647	252	0.389	1171
14.7	17 253	16 979	16 853	16 713	3.87	2137	669	257	0.384	1207
16.5	17 244	16 973	16 839	16 691	3.65	2117	699	266	0.381	1259
20.1	17 237	16 984	16 833	16 672	3.34	2054	763	297	0.389	1381
25.0	17 231	17 013	16 828	16 638	3.32	1956	904	350	0.387	1635
30.6	17 230	17 027	16 828	16 612	3.38	1860	1003	366	0.365	1789
38.3	17 227	17 053	16 830	16 585	3.20	1711	1124	394	0.351	1990
(b) Decreasing pressure										
34.7	17 237	17 001	16 832	16 651	3.34	1885	856	326	0.381	1542
27.3	17 242	16 984	16 839	16 680	3.60	1995	753	288	0.382	1358
21.8	17 249	16 987	16 844	16 692	3.72	2007	733	287	0.392	1329
18.4	17 251	16 983	16 850	16 701	3.88	2055	706	268	0.379	1271
8.7	17 264	16 996	16 873	16 737	4.54	2088	657	255	0.388	1189
3.1	17 276	16 998	16 888	16 776	5.06	2130	563	233	0.414	1035
0.6	17 277	16 976	168 90	16 785	5.77	2139	500	183	0.366	893

$^5D_0$ level in PKBAEu glass at different pressures. Figure 7 shows the variation of lifetime of the $^5D_0$ level of Eu^{3+} ions in PKBAEu glass under pressure. These lifetimes were evaluated from the simple exponential behaviour of the decay curves [32, 33]. From figure 7 and table 1, it is evident that the lifetime of the $^5D_0$ level remains almost constant up to 5 GPa, though the CF strength increases in this pressure range. Beyond 5 GPa the lifetime decreases with increasing pressure, a behaviour generally observed for Ln ions [5, 16, 30, 34]. The decay of the $^5D_0$ level is purely radiative as there is a large energy gap of around 12 200 cm^{-1} between $^5D_0$ and the next lower level $^7F_6$, indicating that the quantum efficiency for the $^5D_0$ level is almost unity. The shortening of lifetime with increasing pressure is attributed to the gradual increase in energy transfer processes, probably enhanced by pressure induced defect centres. A detailed review of such processes is given in [5]. In general, either an increase of the multi-phonon de-excitation probability or an increase of the electronic transition probability can explain the observed decrease of lifetimes under pressure. While the first process can be excluded here because of the large energy gap between the $^5D_0$ and ^7F_J levels, the latter effect is easily explained by the increase in CF strengths around the Eu^{3+} ions with pressure. This results in an enhanced configuration interaction leading to a mixing of opposite parity configurations with the 4f^6 configuration, due to the odd-parity CF Hamiltonians, causing the observed increase in the transition probabilities. This type of behaviour has also been noticed in the case of Sm^{3+} and other Ln^{3+} ions in crystalline solids [35].

As is seen from figure 7, the release of pressure has a significant hysteresis effect on the lifetime, even though the crystal-field strength has reversible nature with pressure. For example,
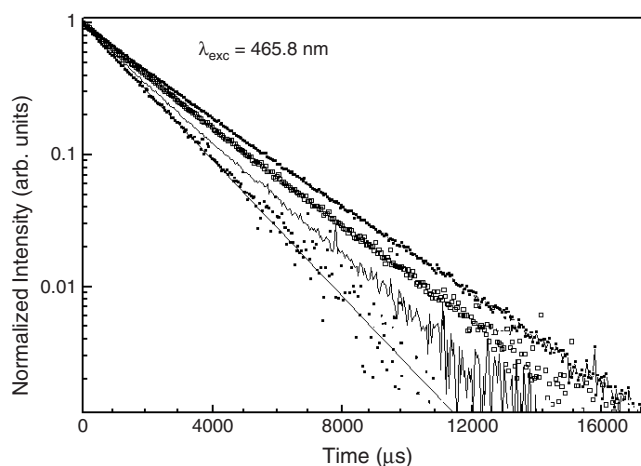
Figure 6. Decay profiles of the $^5D_0$ level of Eu^{3+} in PKBAEu glass at various pressures, starting from above with 0 GPa and going continuously to 12.0, 25.0, and 38.3 GPa. A single exponential fit is included for the decay curve at 38.3 GPa.
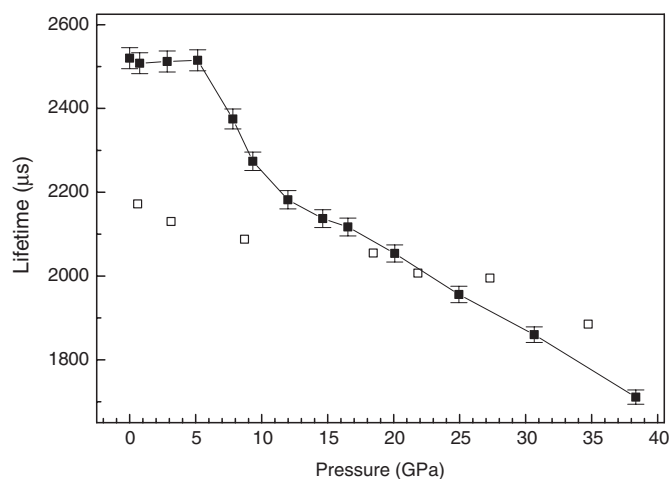

Figure 7. The variation of lifetimes for the $^5D_0$ level of Eu^{3+} ions in PKBAEu glass with pressure. The solid (open) symbols correspond to data taken at increasing (decreasing) pressure and the solid line gives a guide to the eye for increasing pressure.

the lifetime at 3.1 GPa (release of pressure) is 2130 μs, whereas at 16.5 GPa (increasing of pressure), it is 2117 μs. This observation, along with the variation of $I_R(2/1)$ (shown in figure 2), suggests that a permanent deformation of the Eu^{3+} ion sites, a densification of the glass matrix, is taking place with the application of high pressure.

5. Conclusions

Luminescence studies of Eu^{3+} doped phosphate glass have been performed under pressures up to 38.3 GPa at room temperature. The relative luminescence intensity ratio of $^5D_0 \rightarrow {}^7F_2$ to $^5D_0 \rightarrow {}^7F_1$ transitions of Eu^{3+} ions is found to decrease with increasing pressure, indicating

a decrease of asymmetry around the Eu^{3+} ions under pressure. The red shift observed for the emission band positions with increasing pressure is attributed to the variations of the electrostatic and spin–orbit coupling parameters. The continuous increase in the magnitude of splitting observed for the $^7F_1$ and $^7F_2$ levels with pressure arises from the variations in the strength and symmetry of the crystal field around the Eu^{3+} ion. The decay curve of the $^5D_0$ level at ambient pressure is perfectly single exponential and this remains the same over the entire pressure range studied. The reduction of lifetime of the $^5D_0$ level at pressures above 5 GPa can be explained by an increase in the electronic transition probabilities arising from the gradual increase in the crystal-field strengths around the Eu^{3+} ions with pressure. The decrease in the lifetime with increasing pressure could also be partially due to enhancement of pressure induced defect centres. The analysis of luminescence properties measured while releasing the pressures suggests that there is a significant structural hysteresis around the Eu^{3+} ion in the glass matrix.

Acknowledgments

References

[1] Suratwala T I, Steele R A, Wilke G D, Campbell J H and Takeuchi K 2000 *J. Non-Cryst. Solids* **263/264** 213
[2] Jiang S, Luo T, Myers M, Myers J, Lucas J and Peyghambarian N 1998 *Proc. SPIE* **3280** 2
[3] Wang J, Song H, Kong X, Peng H, Sun B, Chen B, Zhang J, Xu W and Xia H 2003 *J. Appl. Phys.* **93** 1482
[4] Liu Z, Qi C, Dai S, Jiang Y and Hu L 2003 *Opt. Mater.* **21** 789
[5] Tröster Th 2003 *Handbook on the Physics and Chemistry of Rare Earths* vol 33, ed K A Gschneidner Jr,
      J-C G Buenzli and V K Pecharsky (Amsterdam: Elsevier) chapter 217
[6] Zhang Q Y, Pita K, Ye W and Que W X 2002 *Chem. Phys. Lett.* **351** 163
[7] Park J K, Lim M A, Kim C H, Park H D, Park J T and Choi S Y 2003 *Appl. Phys. Lett.* **82** 683
[8] Wu C, Qin W, Qin G, Zhao D, Zhang J, Huang S, Lu S, Liu H and Lin H 2003 *Appl. Phys. Lett.* **82** 520
[9] Liu H G, Lee Y I, Park S, Jang K and Kim S S 2004 *J. Lumin.* **110** 11
[10] Görller-Walrand C and Binnemans K 1996 *Handbook on the Physics and Chemistry of Rare-Earths* vol 23,
      ed K A Gschneidner Jr and L Eyring (Amsterdam: Elsevier) chapter 155
[11] Capobianco J A, Proulx P P and Raspa N 1989 *Chem. Phys. Lett.* **160** 591
[12] Zambelli M, Abril M, Lavin V, Speghini A and Bettinelli M 2004 *J. Non-Cryst. Solids* **345/346** 386
[13] Holzapfel W B 2003 *J. Appl. Phys.* **93** 1813
[14] Wybourne B G 1965 *Spectroscopic Properties of Rare Earth Compounds* (New York: Interscience)
[15] Lavin V, Babu P, Jayasankar C K, Martin I R and Rodriguez V D 2001 *J. Chem. Phys.* **115** 10935
[16] Jayasankar C K, Ramanjaneya Setty K, Babu P, Tröster Th and Holzapfel W B 2004 *Phys. Rev. B* **69** 214108
[17] Brecher C and Riseberg L A 1976 *Phys. Rev. B* **13** 81
[18] Auzel F 1979 *Mater. Res. Bull.* **14** 223
[19] Surendra Babu S, Babu P, Jayasankar C K, Sievers W, Tröster Th and Wortmann G 2005 *J. Lumin.* Communicated
[20] Gatterer K, Pucker G and Fritzer H P 1997 *Phys. Chem. Glasses* **38** 293
[21] Oomen E W J L and van Dongen A M A 1989 *J. Non-Cryst. Solids* **111** 205
[22] Chen G, Haire R G and Peterson J R 1995 *J. Phys. Chem. Solids* **56** 1095
[23] Nageno Y, Takebe H, Morinaga K and Izumitani T 1994 *J. Non-Cryst. Solids* **169** 288
[24] Reisfeld R, Zigansky E and Gaft M 2004 *Mol. Phys.* **102** 1319
[25] Ebendorff-Heidepriem H and Ehrt D 1996 *J. Non-Cryst. Solids* **208** 262
[26] Souza Filho A G, Freire P T C, Guedes I, Melo F E A, Mendes Filho J, Custodio M C C, Lebullenger R and
      Hernandes A C 2000 *J. Mater. Sci. Lett.* **19** 135
[27] Jovanic B R 2001 *J. Lumin.* **92** 161

[28] Chen G, Stump N A, Haire R G, Burns J B and Peterson J R 1994 *High Pressure Res.* **12** 83
[29] Jayasankar C K, Richardson F S and Reid M F 1989 *J. Less-Common Met.* **148** 289
[30] Linares C, Louat A and Blanchard M 1977 *Struct. Bonding* **33** 179
[31] Chang N C, Gruber J B, Leavitt R P and Morison C A 1982 *J. Chem. Phys.* **76** 3877
[32] Jayasankar C K, Surendra Babu S, Babu P, Sievers W, Tröster Th and Wortmann G 2004 *J. Phys.: Condens. Matter* **16** 7007
[33] Adam J L, Guimond Y, Jurdyc A M, Griscom L, Mugnier J and Jacquier B 1998 *Proc. SPIE* **3280** 31
[34] Lochhead M J and Bray K L 1995 *Phys. Rev.* B **52** 15763
[35] Lavin V, Martin I R, Jayasankar C K and Tröster Th 2002 *Phys. Rev.* B **66** 064207